Extensive investigation of 0^+ states in rare earth region nuclei

D. A. Meyer,[1,7] V. Wood,[1] R. F. Casten,[1] C. R. Fitzpatrick,[1,2] G. Graw,[3] D. Bucurescu,[4] J. Jolie,[5] P. von Brentano,[5] R. Hertenberger,[3] H.-F. Wirth,[6] N. Braun,[5] T. Faestermann,[6] S. Heinze,[5] J. L. Jerke,[1] R. Krücken,[6] M. Mahgoub,[6] O. Möller,[5] D. Mücher,[5] and C. Scholl[5]

[1]*Wright Nuclear Structure Laboratory, Yale University, New Haven, Connecticut 06520-8124, USA*

[2]*University of Surrey, Guildford, United Kingdom*

[3]*Department für Physik, Ludwig-Maximilians-Universität München, D-85748 Garching, Germany*

[4]*National Institute of Physics and Nuclear Engineering, Bucharest, Romania*

[5]*Institut für Kernphysik, Universität zu Köln, D-50937 Köln, Germany*

[6]*Physik Department, Technische Universität München, D-85748 Garching, Germany*

[7]*Department of Physics, Rhodes College, Memphis, Tennessee 38112-1690, USA*

(Received 11 June 2006; published 24 October 2006)

The nature of 0^+ excitations, especially in transitional and deformed nuclei, has attracted new attention. Following a recent experiment studying ^{158}Gd, we investigated a large group of nuclei in the rare-earth region with the (p,t) pickup reaction using the Q3D magnetic spectrograph at the University of Munich MP tandem accelerator laboratory. Outgoing tritons were recorded at various lab angles, and their angular distributions are compared to those calculated using the distorted-wave Born approximation. Using the unique shape of the $L=0$ angular distribution, more than double the number of 0^+ states than were previously known are identified. The distribution of 0^+ energies and cross sections is discussed in terms of collective and noncollective degrees of freedom, and the density of low-lying 0^+ states is discussed as a corroboration of a characteristic feature of phase transition regions. The degree of level mixing, as extracted from Brody distribution fits to the energy spacings of adjacent 0^+ levels, is also explored.

DOI: 10.1103/PhysRevC.74.044309 PACS number(s): 21.10.Re, 24.10.Eq, 25.40.Hs, 27.70.+q

I. INTRODUCTION

The rare-earth region, with many well-deformed and transitional nuclei, is an ideal venue for the study of the origins of deformation and collective motion. A number of collective modes and quadrupole excitations can form 0^+ states. Probably because of this, such states are often complex and remain poorly understood. Recently, 0^+ excitations have attracted new attention. An experiment [1] measuring 0^+ states in ^{158}Gd by way of the (p,t) transfer reaction discovered seven new 0^+ states and confirmed six previously known below an excitation energy of 3.1 MeV. This was the first observation of such a large number of excited 0^+ states in a deformed nucleus. Experiments involving other nuclei, such as those in the actinide [2] and rare-earth regions, can show whether such a large number of 0^+ excitations in this energy range is widespread or anomalous and can ascertain the energy distribution of 0^+ states along with trends in those distributions with N and Z. In ^{232}U, ^{230}Th, and ^{228}Th [2], several 0^+ states were observed that had not been identified in previous experiments. Unexpectedly large accumulated transfer strengths, more than 60% of the strength of the ground state, were observed, emphasizing the need for microscopic calculations. With an empirical mapping of 0^+ states in nuclei, the regional evolution with N and Z may become apparent, initial structural interpretation can begin, and theory will be challenged to account for these states. For example, following the experimental observations in ^{158}Gd, calculations [3] reproduced the number of 0^+ states. These calculations and calculations like these have become a topic of much discussion [4,5].

Similar data for a large number of nuclei, spanning this mass region and exhibiting a variety of structures, will offer a more thorough test of theory than a single nucleus. Therefore, we examined 16 nuclei spanning the rare-earth region: ^{152}Gd, ^{154}Gd, ^{158}Gd (revisited), ^{162}Dy, ^{168}Er, ^{170}Yb, ^{176}Hf, ^{180}W, ^{184}W, ^{190}Os, ^{192}Pt, ^{194}Pt, ^{196}Hg, ^{198}Hg, ^{200}Hg, and ^{202}Hg. These nuclei have very different classifications (i.e., transitional, deformed, γ-soft, and spherical) as indicated in Fig. 1. In choosing structurally different nuclei, information about trends and types of possible 0^+ excitations can be gained. This article discusses results for ^{152}Gd, ^{154}Gd, ^{162}Dy, ^{168}Er, ^{176}Hf, ^{180}W, ^{184}W, and ^{190}Os and includes those of Ref. [1] for ^{158}Gd.

II. EXPERIMENT AND RESULTS

This series of (p,t) experiments was performed at the University of Munich MP tandem accelerator laboratory using the Q3D [6] magnetic spectrograph. A beam of 25 MeV unpolarized protons was incident on 16 different isotopically enriched targets, and outgoing tritons were measured at laboratory angles of 5°, 17.5°, and 30° with respect to the beam axis. The spectrograph is an ideal instrument for the measurement of transfer reaction products. The 1-m-long focal plane detector [7] has 4–6 keV resolution for 15- to 20-MeV tritons. With such fine resolution and little or no background, very clean cross section measurements down to a few μb/sr were possible. Typical spectra obtained at 5° from ^{192}Os $(p,t)^{190}$Os, ^{178}Hf $(p,t)^{176}$Hf, and ^{154}Gd $(p,t)^{152}$Gd are shown in Fig. 2. We collected data for each target up to ~3 MeV in excitation energy by taking two consecutive

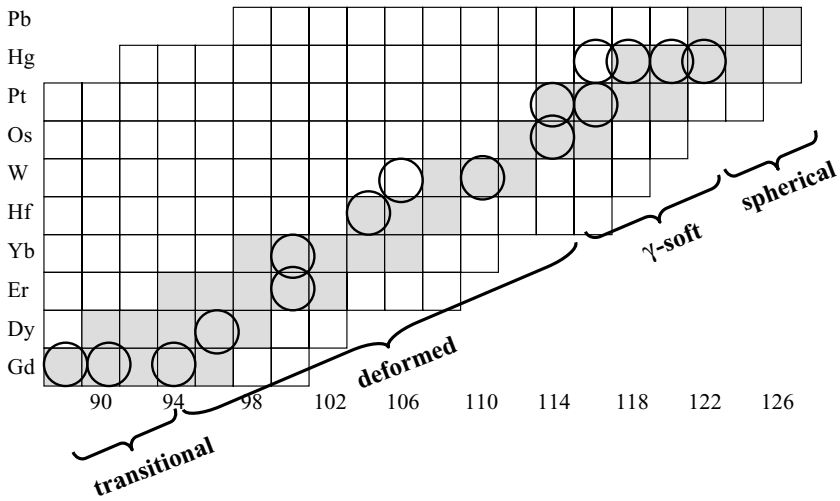

FIG. 1. A portion of the nuclear chart showing nuclei studied in this series of experiments. Circles indicate the residual nucleus in the (p, t) experiments, not the target nucleus.

spectra, each with an energy bin of $\sim$1.7 MeV, at each angle. (A small overlapping portion of the energy range was measured in both spectra.) After normalization to beam current on target, we can effectively combine the two spectra to give one continuous spectrum up to $\sim$3 MeV. Spectra were analyzed using RADWARE [8], and energy calibrations were constructed using known levels in each nucleus. Peaks arising from target impurities were identified using the Q values of possible reactions and information about the targets' isotopic composition.

Spin-parity values of 0^+ states were assigned using the triton angular distributions. 0^+ states can be easily selected from other states because the $L = 0$ transfer angular distribution peaks strongly at forward angles. We compared relative cross sections to those predicted by the distorted-wave Born approximation (DWBA) using the CHUCK3 code [9]. The values for the real and imaginary potentials used in the DWBA calculations were obtained according to Ref. [10].

0^+ states were identified based primarily on the drop in relative cross section between 5° and 17.5°. This drop can be dramatic—more than an order of magnitude—and is unique to $L = 0$ transfers. In contrast, as seen in Fig. 3, angular distributions for higher spins peak at more backward angles.

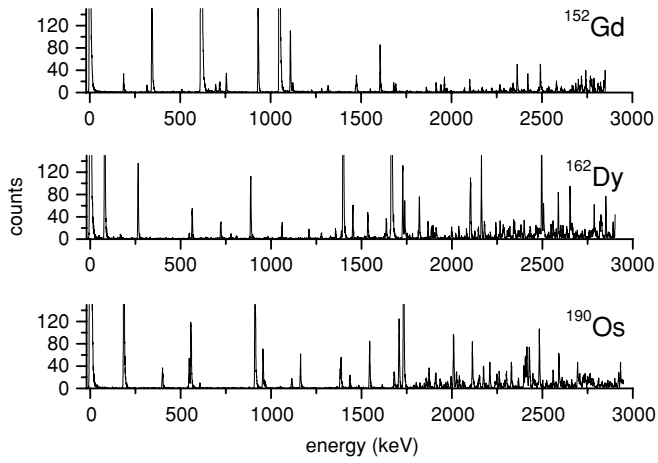

FIG. 2. Typical (p, t) spectra obtained at 5°.

Coupled-channel effects impact cross sections primarily at large angles and can alter $L \neq 0$ angular distributions. However, for $L = 0$ cases, the main effect is only to moderately modify the cross sections at 17.5° and 30°. This has little effect on the forward peak for $L = 0$ transfer, which is therefore a robust empirical signature. Note that although the magnitudes of the predicted DWBA cross sections as well as the location of the minima can vary with the neutron orbital chosen for the calculations, given the N and Z of the target and the Q value, it is a minor effect for $L = 0$ transfer. To elaborate on the angular distributions, 0^+ states assigned in this work for ^{154}Gd, ^{176}Hf, and ^{190}Os are shown in Figs. 4, 5, and 6 with their corresponding DWBA predictions.

Figure 7 shows the initial drop in cross section for 0^+ states and the different behavior of the first 2^+ and 4^+ states of the ground and γ bands by plotting the ratio of the cross sections at 5° and 17.5° versus the ratio of the cross sections at 17.5° and 30°. The ratio of the cross sections between 5° and 17.5° is large (as high as $\sim$60) for $L = 0$ transfer, whereas it is generally less than 3 for known 2^+ and 4^+ states of the ground and γ bands. In most cases, the cross-section ratio between 17.5° and 30° is greater than $\sim$1 for known $L = 2$ transfers, greater than 0.5 for known $L = 4$ transfers, and less than 0.5 for known $L = 0$ cases (known 0^+ states). This does not provide a clean separation of the 0^+ states from 2^+ and 4^+ states and,

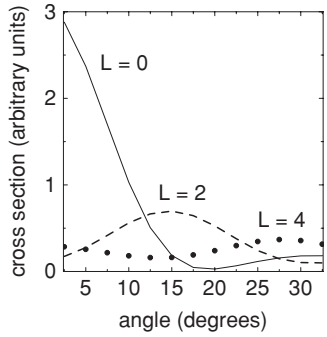

FIG. 3. Angular distributions calculated using the DWBA for $L = 0, 2, 4$ transfer. Calculations have been normalized to the same total reaction cross section calculated by the DWBA.

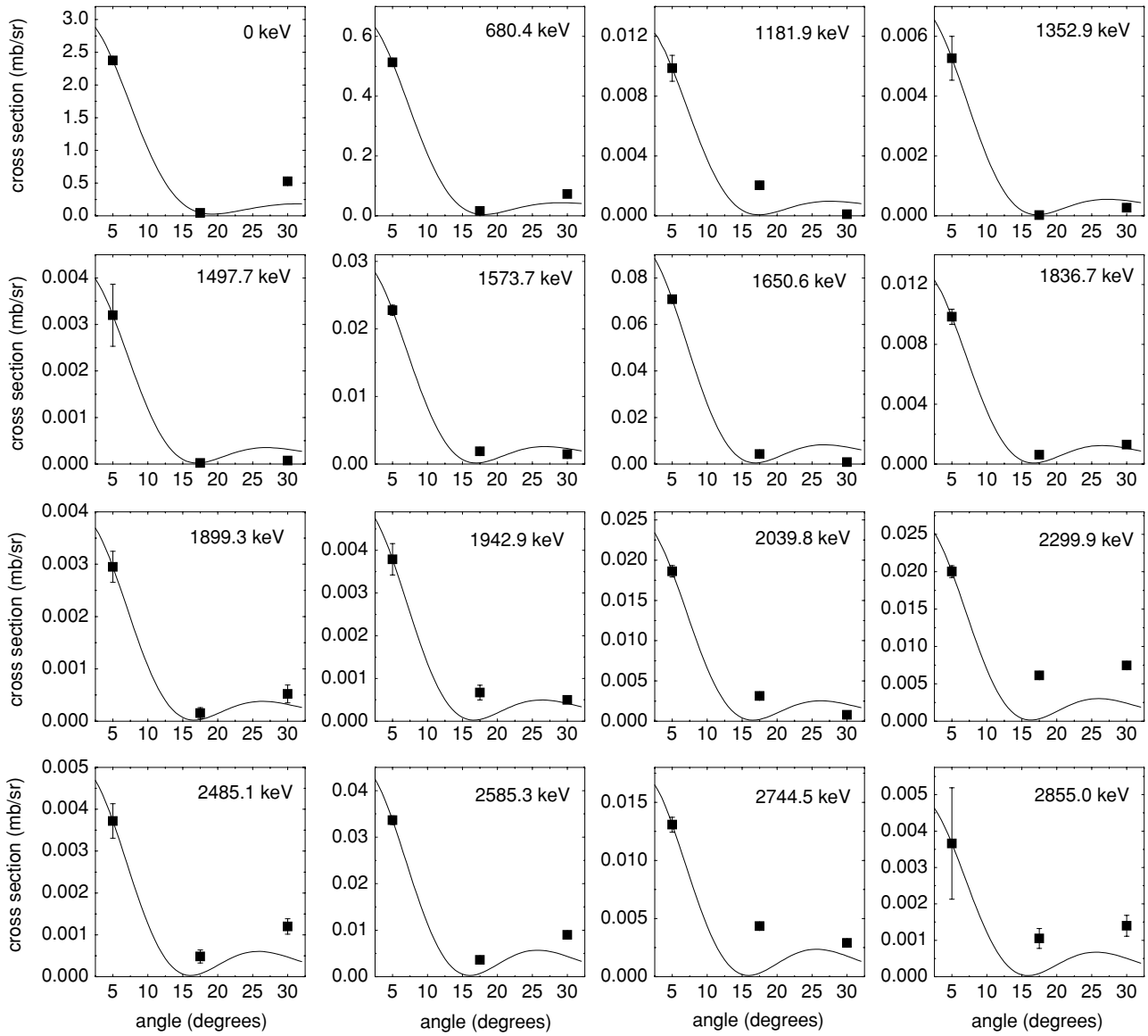

FIG. 4. Angular distributions for observed 0^+ states in ^{154}Gd. Data (points) are compared to DWBA calculations (line). The DWBA calculations for $L = 0$ transfers are normalized to the data at 5°.

therefore, emphasis was placed on the drop in cross section between 5° and 17.5° when making 0^+ assignments.

Coupled-channel effects can affect $L = 0$ transfer only if the 5° cross sections are very small. Then, at 17.5°, where the direct cross section is even smaller for 0^+ states, the contribution from coupled-channel effects will nearly always raise the measured cross section, reducing the ratio $\sigma(5^o)/\sigma(17.5^o)$. We see this effect in Fig. 8, which shows the ratio of the cross sections at 5° and 17.5° against the cross section at 5°. Low ratios are clearly associated with small absolute cross sections, as seen in the magnified view on the right. Not surprisingly, therefore, the majority of the tentatively assigned 0^+ states—tentative because of a smaller drop in cross section between 5° and 17.5° —also have small absolute cross sections. (The three exceptions are the states at 967.4 keV in ^{176}Hf, 774.2 keV in ^{162}Dy, and 1865.6 keV in ^{176}Hf. The first two are tentative assignments based on their extremely low excitation energies. The latter is tentatively assigned because although it exhibits a large drop in cross section between 5° and 17.5°, its angular distribution does not fit the DWBA calculation very well.)

In the nuclei discussed here, a total of ninety-nine 0^+ states were assigned: 70 of these are new, and 22 of these are tentative. (These data are slightly updated from those in Ref. [11] due to further investigation of ^{168}Er [12].) A number of other states with rather small ratios of cross sections between 5° and 17.5° were known to correspond to $J \neq 0^+$ states. Table I lists the energies and cross sections at 5°, 17.5°, and 30°, for the 0^+ states observed in this work. Only one previously observed 0^+ state was not seen. This state, in ^{154}Gd at 1295 keV, was proposed [13] based on an E0 transition and the E4 component of a doubly placed γ transition. We determine an

TABLE I. Energies and cross sections at 5°, 17.5°, and 30° for observed 0^+ states.

	Energy (keV)	Cross section (mb/sr)		
		5°	17.5°	30°
^{152}Gd	0.0[a]	0.913(4)	0.0171(4)	0.205(1)
	614.8(4)[a]	1.080(5)	0.0199(4)	0.209(1)
	1048.0(4)[a]	0.506(3)	0.0111(4)	0.0761(7)
	1680.5(5)	0.0058(4)	0.0014(1)	0.0021(1)
	1961.9(5)[b]	0.0077(5)	0.0015(1)	0.0007(1)
	2363.2(6)	0.0122(6)	0.0007(1)	0.0015(1)
	2421.5(7)	0.0080(5)	0.0006(1)	0.0010(1)
	2491.9(7)[b]	0.0021(7)	0.0008(1)	0.0020(2)
	2579.8(7)	0.0050(4)	0.0016(1)	0.0016(1)
	2767.7(7)	0.0071(6)	0.0015(2)	0.0023(2)
	2810.2(7)	0.0039(5)	0.0007(2)	0.0013(2)
^{154}Gd	0.0[a]	2.37(1)	0.045(1)	0.526(3)
	680.4(3)[a]	0.513(2)	0.0161(6)	0.0729(6)
	1181.9(3)[a]	0.0099(9)	0.0020(3)	0.0001(1)
	1352.9(3)	0.0053(7)	0.00002(9)	0.0003(1)
	1497.7(3)	0.0032(7)	0.00002(9)	0.0001(1)
	1573.7(3)[a]	0.0228(8)	0.0019(2)	0.0015(1)
	1650.6(4)[a]	0.071(1)	0.0043(3)	0.0008(1)
	1836.7(4)	0.0099(5)	0.0006(2)	0.0013(1)
	1899.3(4)	0.0030(3)	0.0002(1)	0.0005(2)
	1942.9(4)	0.0038(4)	0.0007(2)	0.0005(1)
	2039.8(4)	0.0186(7)	0.0031(3)	0.0008(1)
	2299.9(5)[b]	0.0200(8)	0.0061(4)	0.0075(4)
	2485.1(5)	0.0037(4)	0.0005(2)	0.0012(2)
	2585.3(5)	0.0337(9)	0.0036(3)	0.0090(4)
	2744.5(5)[b]	0.0131(6)	0.0044(3)	0.0029(2)
	2855.0(5)[b]	0.004(2)	0.0011(3)	0.0014(3)
^{162}Dy	0.0[a]	0.878(5)	0.0262(6)	0.290(5)
	774.2(3)[c]	0.0011(2)	0.0001(1)	0.0005(1)
	1398.9(3)[a]	0.093(2)	0.0020(2)	0.0229(8)
	1666.3(4)[a]	0.276(3)	0.0118(5)	0.046(1)
	1814.6(5)	0.0016(2)	0.0003(1)	0.0005(1)
	1820.3(5)	0.0115(5)	0.0010(1)	0.0010(2)
	2126.5(6)[a]	0.0016(2)	0.0013(2)	0.0011(1)
	2496.7(7)	0.0283(7)	0.0036(3)	0.0028(2)
	2588.8(7)	0.0104(4)	0.0018(2)	0.0040(3)
	2655.3(7)	0.0121(5)	0.0028(4)	0.0018(3)
	2663.0(7)[b]	0.0027(3)	0.0009(4)	0.0025(3)
	2802.9(7)[b]	0.0016(2)	0.0005(2)	0.0012(2)
^{168}Er	0.0[a]	0.693(10)	.0276(6)	0.268(4)
	1217.3(1)[a]	0.0104(5)	0.0018(2)	0.0054(3)
	1421.8(1)[a]	0.0095(5)	0.0006(1)	0.0039(3)
	1833.4(2)[a]	0.0067(4)	0.0005(1)	0.0020(2)
	2114.8(3)	0.0021(2)	0.00014(7)	0.00055(9)
	2200.6(2)		0.00007(13)	0.0003(1)
	2366.2(2)	0.0174(6)	0.0012(2)	0.0034(2)
	2392.1(2)[b]	0.0052(3)	0.0014(2)	0.0019(1)
	2572.5(2)	0.0786(12)	0.0053(3)	0.0226(6)
	2617.4(2)	0.0344(9)	0.0007(1)	0.0075(3)
	2643.8(2)[b]	0.0020(3)	0.0010(2)	0.0012(2)
	2789.1(7)	0.0114(6)	0.0027(2)	0.0053(3)
	2842.1(5)	0.042(1)	0.0013(2)	0.0099(4)
	2872.2(5)	0.044(1)	0.0018(3)	0.0095(4)
	2947.4(10)	0.061(1)	0.0090(5)	0.0139(5)

TABLE I. *(Continued.)*

	Energy (keV)	Cross section (mb/sr)		
		5°	17.5°	30°
^{176}Hf	0.0[a]	0.817(6)	0.0239(5)	0.255(2)
	967.4(3)[c]	0.0054(3)	0.0003(1)	0.0012(1)
	1150.1(3)[a]	0.109(2)	0.0057(2)	0.0340(7)
	1196.7(4)	0.0042(3)	0.0006(1)	0.0012(1)
	1293.3(5)[a]	0.086(2)	0.0045(2)	0.0256(5)
	1499.2(5)	0.0008(1)	0.0001(1)	0.0003(1)
	1746.3(6)[a]	0.067(1)	0.0038(2)	0.0189(5)
	1865.6(6)[b]	0.0006(1)	0.0001(1)	0.0009(2)
	2340.4(7)	0.0084(3)	0.0028(2)	0.0037(2)
	2445.2(7)[b]	0.0201(6)	0.0083(6)	0.0093(5)
	2489.8(7)	0.0062(3)	0.0014(2)	0.0018(1)
^{180}W	0.0[a]	1.113(6)	0.0514(8)	0.363(2)
	1037.6(3)[c]	0.0006(1)	0.0003(1)	0.0003(1)
	1380.8(3)	0.0031(4)	0.0004(1)	0.0010(1)
	1472.1(4)[b]	0.0008(2)	0.0002(1)	0.0003(1)
	1513.6(4)[a]	0.110(1)	0.0109(3)	0.0351(6)
	1689.4(5)	0.022(1)	0.0019(2)	0.0072(4)
	1768.4(5)	0.0163(5)	0.0031(2)	0.0072(3)
	1932.3(6)[b]	0.0080(5)	0.0034(2)	0.0023(2)
	2036.7(6)	0.0213(6)	0.0010(1)	0.0047(2)
	2181.6(6)	0.0024(6)	0.0001(1)	0.0017(4)
	2326.8(7)	0.011(2)	0.0018(3)	0.0024(7)
^{184}W	0.0[a]	1.134(9)	0.0367(7)	0.371(2)
	1003.3(4)[a]	0.083(2)	0.0022(5)	0.0310(6)
	1614.3(5)	0.0121(5)	0.0009(1)	0.0035(2)
	1774.5(5)	0.0028(2)	0.0007(1)	0.0007(1)
	1795.8(5)	0.0081(4)	0.0022(2)	0.0028(2)
	2030.7(6)	0.0033(3)	0.0004(1)	0.0012(1)
	2111.2(6)	0.0252(7)	0.0057(3)	0.0116(3)
	2309.6(7)[a]	0.0077(4)	0.0034(2)	0.0034(2)
	2404.7(7)	0.0119(5)	0.0029(2)	0.0051(2)
	2468.9(7)[b]	0.0048(3)	0.0021(7)	0.0025(5)
	2512.7(7)	0.007(1)	0.0017(4)	0.0048(5)
	2567.9(7)[b]	0.0102(7)	0.0049(3)	0.0053(3)
	2826.4(7)	0.0370(9)	0.0082(3)	0.0163(4)
	2871.3(7)[b]	0.0123(6)	0.0048(3)	0.0057(2)
	2927.7(7)[b]	0.0076(5)	0.0028(3)	0.0035(2)
	2939.6(7)[b]	0.0050(4)	0.0021(2)	0.0025(2)
^{190}Os	0.0[a]	1.54(1)	0.070(2)	0.555(6)
	911.9(3)[a]	0.074(2)	0.0044(3)	0.0262(9)
	1382.5(3)	0.0072(7)	0.0031(9)	0.0045(6)
	1545.2(4)[a]	0.027(1)	0.0043(3)	0.0104(4)
	1733.0(4)[a]	0.115(2)	0.0120(5)	0.0421(8)
	1956.6(4)	0.0015(2)	0.0004(1)	0.0004(1)
	2483.5(5)	0.0236(9)	0.0063(6)	0.0112(4)

[a]Previously known 0^+ state.
[b]Tentative assignment.
[c]Probable contaminant not identified.

upper limit of 0.0005 mb/sr for the cross section at 5° for this state. Table II gives the number of assignments by nucleus and comparison with previously known 0^+ states. The number of 0^+ states in these nuclei is at least double that previously reported: typically from 2–4 previously known states to 7–16 observed in this work.

III. DISCUSSION

Although complete structural understanding of the nature of these states requires additional experiments, knowledge of the number and excitation energies of the 0^+ states and their relative strengths is already an important first step both to

TABLE II. Number of 0^+ states obtained in this work. Observed 0^+ states include both tentative and previously known states.

	Observed 0^+ states	Tentative 0^+ states	Previously known 0^+ states	Previously known 0^+ states not observed
^{152}Gd	11	2	3	0
^{154}Gd	16	3	6	1
^{162}Dy	12	3	4	0
^{168}Er	15	2	4	0
^{176}Hf	11	3	4	0
^{180}W	11	3	3	0
^{184}W	16	6	2	0
^{190}Os	7	0	3	0
Total	99	22	29	1

identify trends in these nuclei and to present a testing ground for theories. The data are collected in Fig. 9. It is interesting to look for possible trends across such a broad range of nuclei. Aside from the large number of 0^+ states discovered, their distribution as a function of excitation energy and their strengths relative to the ground state vary considerably from nucleus to nucleus as shown in the figure. For instance, ^{158}Gd and ^{180}W have a fairly even distribution of 0^+ states, whereas ^{162}Dy appears to have fewer low-lying 0^+ states and clusters of 0^+ states at higher energies. Startling variations in the number and distribution of 0^+ states are apparent when comparing, for example, ^{184}W and ^{190}Os or ^{180}W and ^{184}W, which differ by only four valence neutrons. These variations alone suggest noncollective origins for many of these states.

Some of the 0^+ states occur at energies as low as $\sim$1200 keV, well below the pairing gaps in these nuclei. The number and variations in the number of 0^+ states below the pairing gap is especially interesting: as high as 10 excited 0^+ states in ^{154}Gd (see discussion below) but relatively constant at $\sim$5 among the other nuclei.

To further pursue the possible collective nature of some of these states, we note that collective 0^+ states can be formed by the antialigned superposition of two-phonon excitations, such as the γ vibration or octupole modes or by combining two $K = 0^+$ excitations [14]. The locations of two-phonon excitations, estimated by doubling the energy of the one-phonon states without regard for anharmonicity, and of known single-phonon modes with $J = 0^+$, are compared to the excitation energies of the observed 0^+ states in Fig. 9. Notice that there are many 0^+ states below any harmonic double-phonon excitations. For example, in ^{158}Gd, there are seven 0^+ states below the lowest estimated harmonic double-phonon excitation, and in ^{184}W

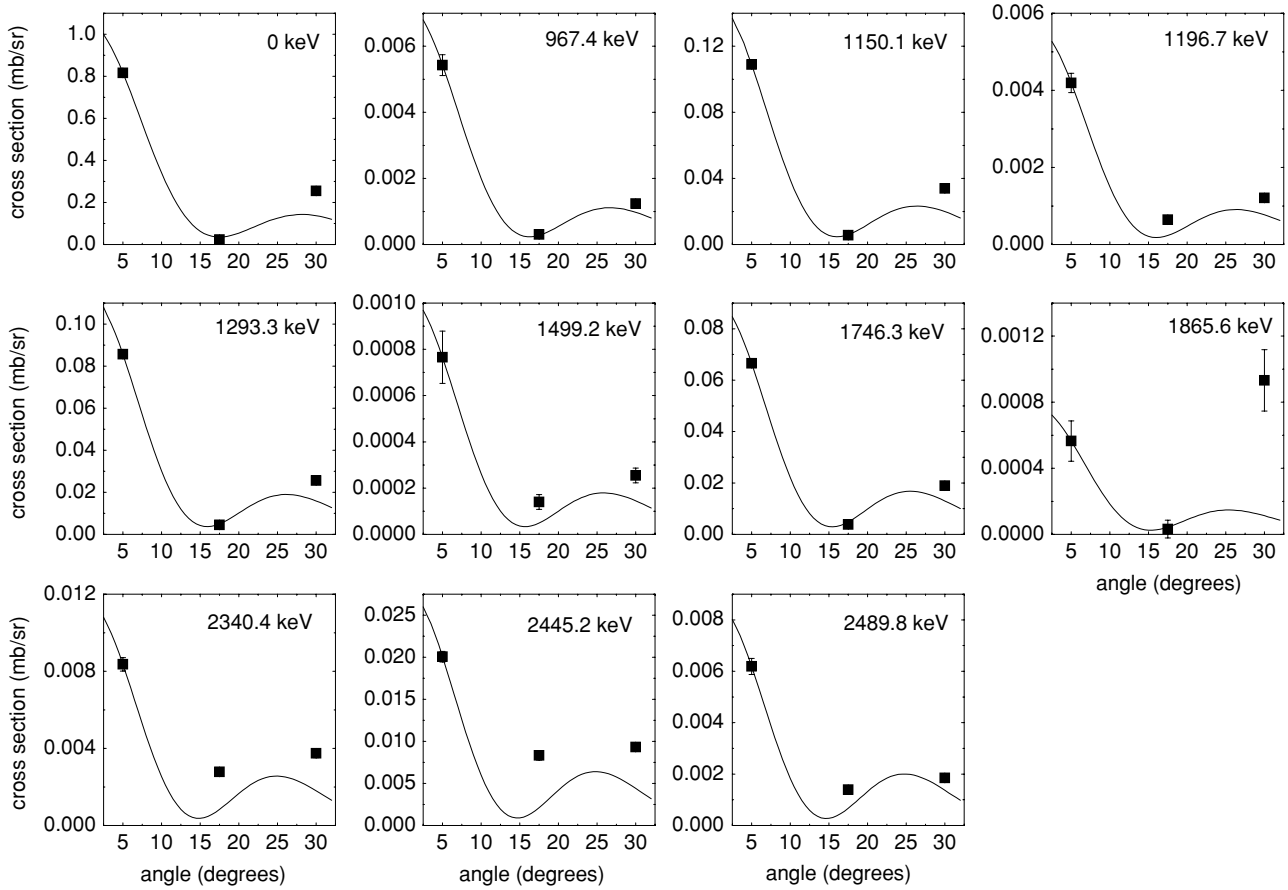

FIG. 5. Angular distributions for observed 0^+ states in ^{176}Hf. Data (points) are compared to DWBA calculations (line). The DWBA calculations for $L = 0$ transfers are normalized to the data taken at 5°.

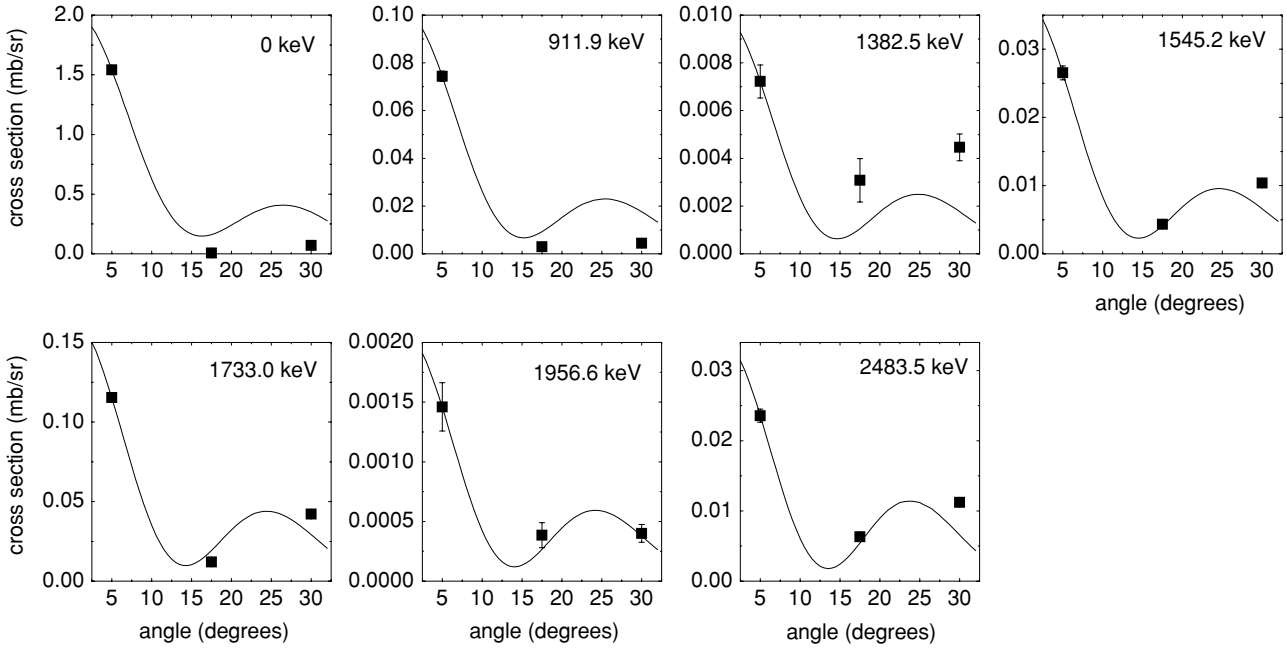

FIG. 6. Angular distributions for observed 0^+ states in ^{190}Os. Data (points) are compared to DWBA calculations (line). The DWBA calculations for $L = 0$ transfers are normalized to the data at 5°.

there are five to seven such states. In ^{168}Er, there are seven 0^+ states below all but one double-phonon energy. The nature of these states is intriguing because they are unlikely to be two-quasiparticle states, yet it is not obvious what collective modes could account for them. When octupole degrees of freedom were incorporated into realistic calculations using the spdf-IBA [15], the number of 0^+ states predicted below 3 MeV in ^{158}Gd is nearly the number observed. If these states can indeed be explained in terms of double octupole phonons, then only a few of the 0^+ states in this energy region are largely two quasiparticle in nature. Another way of looking at this is to note that, frequently, there are a number of 0^+ states below the pairing gap (dashed vertical lines in Fig. 9). We return to this point later.

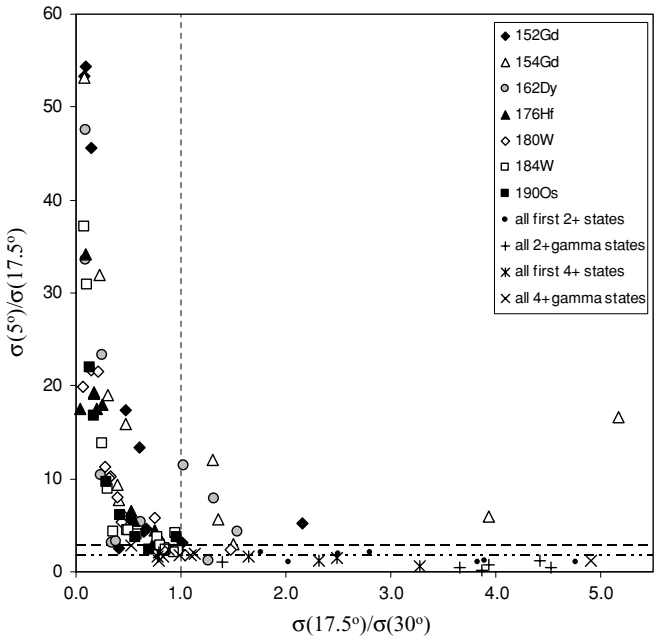

FIG. 7. Ratios of cross sections for 0^+ states observed in this work compared with the ratios for the 2^+ and 4^+ states of the ground and γ bands. The horizontal dashed line at $\sigma(5^\circ)/\sigma(17.5^\circ) = 3$ gives the limit for definite 0^+ assignments, whereas the dash-dot-dotted line at $\sigma(5^\circ)/\sigma(17.5^\circ) = 2$ gives the limit for tentative 0^+ assignments. The vertical line at $\sigma(17.5^\circ)/\sigma(30^\circ) = 1$ divides the plot into angular distributions that rise (<1) and fall (>1) between 17.5 and 30°.

The possible double-phonon nature can be explored by looking at known γ decay from 0^+ states. However, very little data of this type are available [16]. Experiments to study the γ-ray decay from 0^+ states, particularly branching ratios and E1 decays to low-lying negative parity states, are needed to further explore this hypothesis. In one case, the strong decay of the band built on the 0^+ state at 1400 keV in ^{162}Dy [17] to the γ band suggests this state has a significant amplitude for a double γ vibration. The 2^+ state in this band lies at 1453.5 keV, decaying to the 4^+ states of the ground and γ bands with transitions of 1187.8 and 392.5 keV, respectively. The relative intensities of these two transitions are 12.7 and 0.18. The value for the square of the reduced matrix element for decay to the γ band is 10 times larger than that for decay to the ground band. In this case, the actual double phonon lies 500 keV below the harmonic estimate, showing that comparison to these double-phonon estimates should be taken only as a starting point for further investigation and that anharmonicities are important.

In all cases except ^{152}Gd, the cross section is dominated by the ground state. Any cross section greater than 10% of the ground state is rare and points to some particular

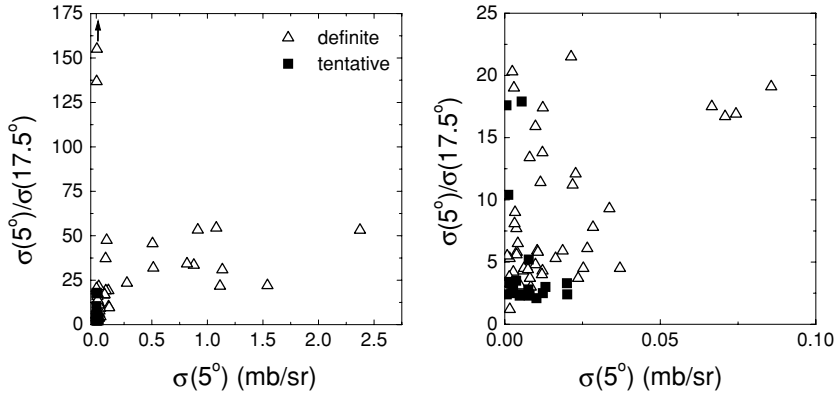

FIG. 8. (Left) The ratio of the cross sections $\sigma(5^\circ)/\sigma(17.5^\circ)$ is shown versus the absolute cross section at 5°. (Right) Expanded plot of the lower left portion of the left panel, showing that small values of $\sigma(5^\circ)/\sigma(17.5^\circ)$ correspond to small absolute cross sections.

structural aspect that should appear in a realistic theoretical interpretation. One situation that can result in large cross sections occurs when the shape of the target ground state and an excited state are similar. This plays a particularly important role in transition regions such as that near $A \sim 150$ [18]. For example, shape coexistence in ^{150}Sm and ^{152}Sm [19] yields strong cross sections for excited 0^+ states. The cross section from the deformed ^{152}Sm ground state to a deformed excited state in ^{150}Sm is enhanced, whereas the cross section to the more spherical ground state of ^{150}Sm is reduced. Similarly, the ground states of even-even Gd isotopes with $A \geqslant 154$ are deformed, whereas the ground states of even-even Gd isotopes with $A < 154$ are spherical. Spherical and deformed shapes coexist in ^{152}Gd and ^{154}Gd [20]. An enhanced cross section from the deformed ^{154}Gd ground state to a deformed excited state in ^{152}Gd is observed. Note that the sum of cross sections (at 5°) of the ground state (0.91 mb/sr) and first excited 0^+ state (1.08 mb/sr) in ^{152}Gd is similar to that of the ground state for neighboring nuclei (e.g., 2.37 mb/sr for the ground state of ^{154}Gd). Detailed microscopic calculations could provide insight into observed cross sections as shape coexistence in certain nuclei cannot account for all of the large cross sections. As seen in Fig. 10, many nuclei have states around 1500 keV with large cross sections. These large cross sections occur below the pairing gap in these nuclei, suggesting some degree of collectivity for these states. In ^{168}Er, unique among the nuclei studied, there are no large cross sections near 1.5 MeV but rather there are significant cross sections near 3 MeV. There is no current explanation for the strength of these cross sections.

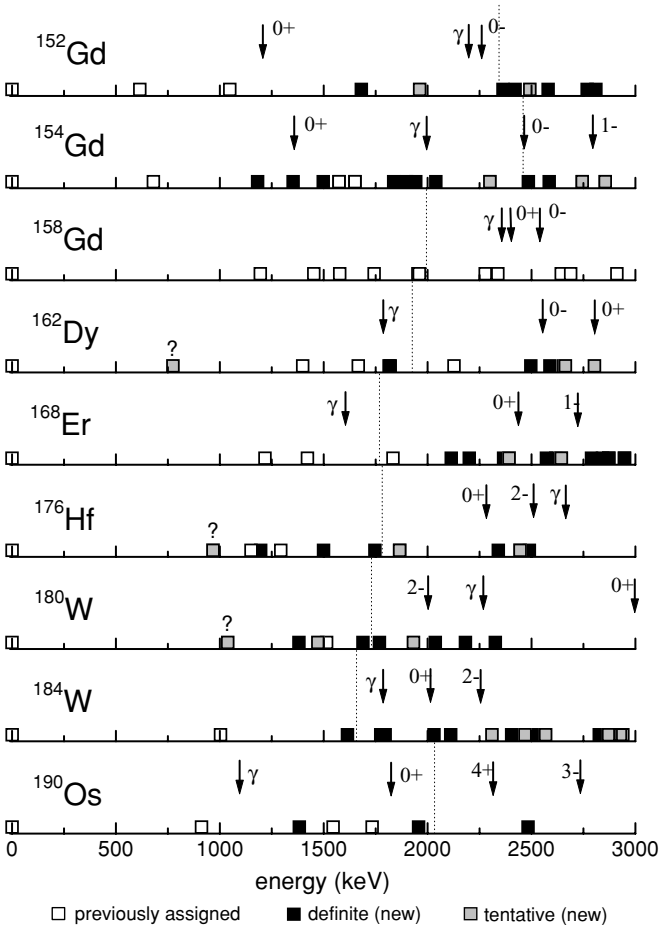

FIG. 9. Locations of 0^+ states obtained in this work. Open symbols indicate previously known states, black symbols indicate new 0^+ states, and gray symbols indicate tentative assignments. Estimated locations of the double phonon states are given by arrows labeled according to the single phonon whose energy was doubled, and the dotted lines indicate the pairing gap for each nucleus calculated from odd-even mass differences. Data for ^{158}Gd taken from Ref. [1].

Following the publication of the data obtained for ^{158}Gd [1], calculations [3] reproduced the number and energies of the observed 0^+ states fairly well. Similar calculations for ^{168}Er [5] also give a reasonable account of the number and energies of the 0^+ states in that nucleus. The present data for these additional nuclei, with variations in number, excitation energy, and cross sections for the 0^+ states, provide a much more stringent test of potential theories. A particular challenge lies in understanding the significant variations with few obvious trends exhibited by the experimental results for nuclei across this region.

We return to the number of 0^+ states and discuss further the role of phase transitional behavior in the number of 0^+ states observed. Figure 11 shows a histogram of the number of definite 0^+ assignments versus excitation energy for these nuclei. We can easily distinguish ^{154}Gd from the other nuclei by the steeper increase in the number of 0^+ states and the larger number of 0^+ states below 3 MeV. One explanation

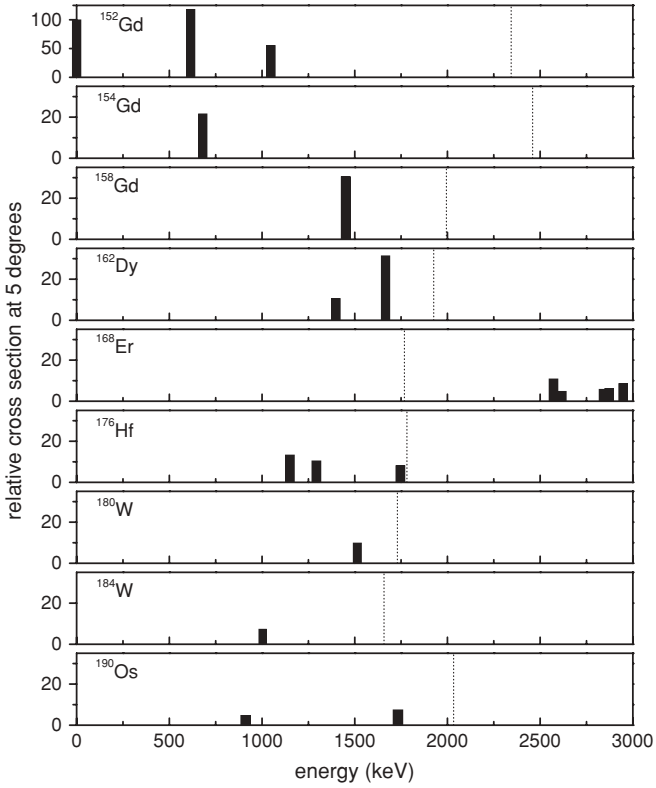

FIG. 10. Relative cross sections at 5° (normalized to 100 for the ground-state cross section) greater than 5% of the ground-state cross section are shown for each nucleus as a function of excitation energy.

of this behavior has been discussed [11]. It is possible that independent sets of states could be built on both the deformed and spherical configurations in a transitional nucleus such as ^{154}Gd, giving rise to a larger number of 0^+ states at low energies in critical point phase-transitional regions. Moreover,

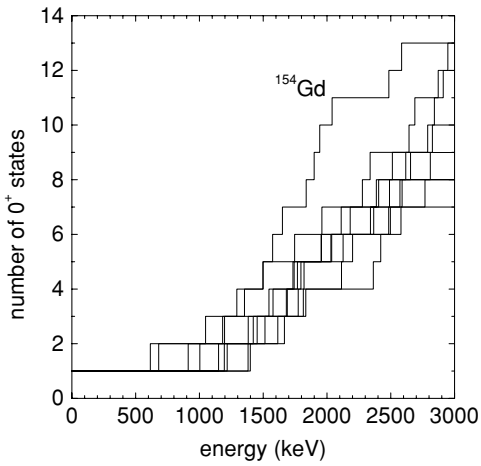

FIG. 11. Histogram showing the number of definitely assigned 0^+ states in each nucleus as a function of excitation energy. Notice ^{152}Gd, ^{158}Gd, ^{162}Dy, ^{168}Er, ^{176}Hf, ^{180}W, ^{184}W, and ^{190}Os follow roughly the same trend. There is a marked increase in the number of 0^+ states at low energies in ^{154}Gd, distinguishing it from the others. (This figure is similar to Fig. 4 in Ref. [11] but reflects updated data available for ^{168}Er according to Ref. [12].)

collective model calculations [21–23] predict a minimum in the energy of the lowest excited 0^+ state in the transition region that is also observed here (see ^{152,154}Gd in Fig. 9).

The behavior of collective 0^+ states near first-order phase transitions has been examined in a series of calculations [24] using the Ising-type IBA Hamiltonian [25] of the consistent Q formalism (CQF) [26]:

$$H = \kappa[(\epsilon/\kappa)n_d - Q \cdot Q] = \alpha\left[\eta n_d - \left(\frac{\eta - 1}{N}\right) Q \cdot Q\right], \tag{1}$$

where

$$Q = (s^\dagger \tilde{d} + d^\dagger s) + \chi(d^\dagger \tilde{d}), \tag{2}$$

where χ ranges from zero for γ-soft nuclei to $-\sqrt{7}/2$ for SU(3). In these calculations, the regime from spherical to deformed is expressed primarily by the parameter η, where $\eta = 0$ indicates a rotor, $\eta = 1$ indicates a vibrator, and $\eta \sim 0.8$ indicates the transition point for large boson number. The results of the calculations of Ref. [24], shown in Fig. 12, reveal both a marked descent of the energy of the first excited 0^+ state and a compression in energy of all excited 0^+ states. The calculations indicate the largest energy density of low-lying 0^+ states should occur in the transition region. These calculations have been carried out using very high boson numbers to highlight the phase-transitional effects.

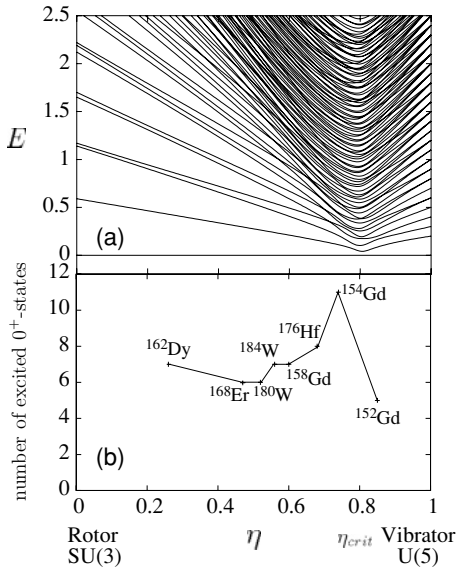

FIG. 12. (Top) Schematic IBA calculations using 30 bosons show a marked increase in the density of 0^+ states in the phase-transitional region. (Bottom) The number of experimentally observed 0^+ states, plotted versus their calculated η values, mirrors the increased density. (This figure is similar to Fig. 1 in Ref. [11] but reflects updated data available for ^{168}Er according to Ref. [12].)

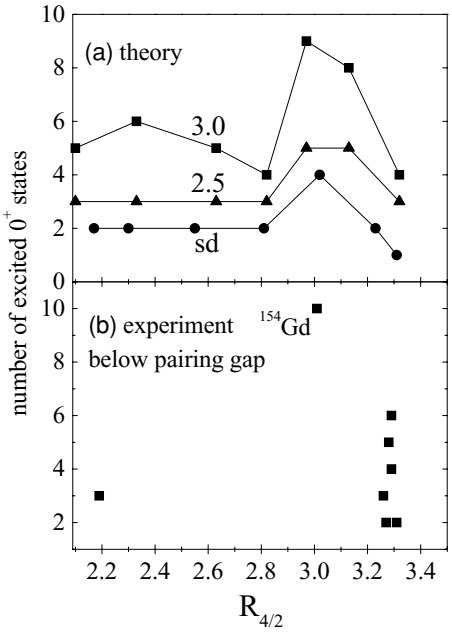

FIG. 13. (a) Predictions from the realistic IBA calculations discussed in the text, plotted against $R_{4/2}$. The curves show the numbers of 0^+ states given by the sd-IBA up to 2.5 MeV and by the spdf-IBA up to 2.5 and 3.0 MeV as labeled. (b) The number of observed 0^+ states below the pairing gap (determined from odd-even mass differences) is shown as a function of $R_{4/2}$. There are nearly twice as many excited 0^+ states in ^{154}Gd below the pairing gap as in any of the other nuclei. (This figure is similar to Fig. 5 in Ref. [11] but reflects updated data available for ^{168}Er according to Ref. [12].)

However, the increased level density in the phase-transitional region persists for lower boson numbers. As pointed out in Fig. 11, ^{154}Gd is easily distinguished from the other nuclei by its excess of 0^+ states, particularly in the energy range from 1.5 to 2.5 MeV. ^{154}Gd has an $R_{4/2}$ value of 3.02, at the critical point of the first-order spherical-deformed phase transition near $A = 150$ [27]. This enhanced density of observed low-lying 0^+ states near the phase-transitional point is the first corroboration of this basic characteristic of a first-order phase transition [11].

Because the calculations shown in the top part of Fig. 12 are schematic, we turn to more realistic calculations presented in two ways. First, many of the nuclei in this study have previously been fit [21] with the IBA using the same Hamiltonian discussed above. The number of observed 0^+ states for each nucleus at the fitted η value is shown in the bottom part of Fig. 12. The nuclei ^{180,184}W were not included in Ref. [21] but have been separately fit [28]: the parameters for ^{180,184}W are $\eta = 0.56$ and 0.52, respectively, and $\chi = -0.58$ and -0.55, respectively. The predicted increase in the number of 0^+ states at low energies at the phase-transitional point is apparent.

In a second approach, also using Eq. (1), calculations have been carried out for a range of parameter values ε/κ and χ for realistic boson numbers $N_B = 6 - 16$. Each calculation reproduces typical values of $E(2^+)$ and the general behavior of intrinsic excitations (e.g., the γ band) in the rare-earth region. The numbers of low-lying 0^+ states from these calculations for selected $R_{4/2}$ values between vibrator and rotor are shown in Fig. 13(a), and we again see the increase at the phase-transition point. However, the sd-IBA predicts far fewer states than are observed experimentally. Calculations incorporating negative parity p and f bosons yield a more realistic number of states in this energy region in the case of ^{158}Gd [15]. Although the experimentally observed states are likely to include quasiparticle excitations that mix with collective excitations, it is interesting to carry out simple spdf-IBA calculations [29] across the range of nuclei from spherical to deformed. To keep the number of additional parameters to a minimum, the p and f boson energies were kept constant at values that reproduce typical negative parity excitations, and calculations were restricted to the U(5) to SU(3) leg of the symmetry triangle. The number of predicted 0^+ states are also included in Fig. 13(a). Naturally, these calculations exhibit many more 0^+ states, closer in number to the experimental observations, and preserve a clear peaking near the phase transition.

The data reflect the increased energy density of 0^+ states near the phase-transitional region. To focus on states more likely to be collective, Fig. 13(b) shows the number of excited 0^+ states below the pairing gap in each nucleus, plotted against $R_{4/2}$. The increase in the number of 0^+ states in the transitional region is again observed.

Observation of the large number of 0^+ states found in this study offers another perspective on structure as well, namely the possibility of an analysis in terms of the ordered or chaotic (mixed) nature of the energy spectra in these nuclei. Information about the degree of mixing of nuclear levels

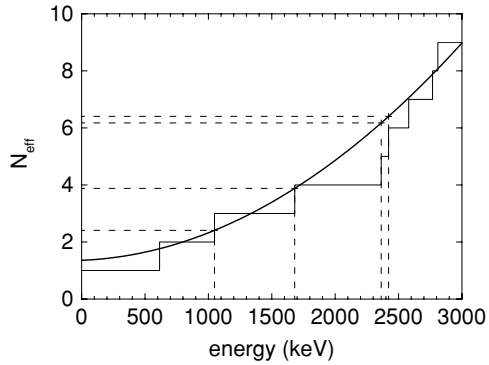

FIG. 14. Histogram of 0^+ energy spacings in ^{152}Gd, showing the method of fitting a quadratic function to the level distribution to extract a normalized effective nearest neighbor spacing distribution, $N_{\rm eff}$.

can be deduced by evaluating the nearest neighbor spacings, the energy difference between levels of the same spin and parity [30]. In the case of strong mixing, we can describe the distribution of nearest neighbor spacings using the Wigner distribution. In the case of small configuration mixing, the Poisson distribution more aptly describes the distribution of nearest neighbor spacings. The Brody distributions describe systems with intermediate degrees of mixing in terms of a parameter ω that ranges from 0 for a Poisson distribution to unity for a Wigner distribution. Because the statistics for one nucleus are very limited, we have fit the Brody distributions to the entire set of nearest neighbor spacings from the nuclei in this work using a standard unfolding method [31,32]. First, a quadratic function was fit to the histogram plot for each nucleus individually in Fig. 11. Then, for each observed level, the value of the fit function was used to generate a spacing distribution, $N_{\rm eff}$, as illustrated in Fig. 14. Notice that small energy spacings correspond to small spacings in $N_{\rm eff}$. The $N_{\rm eff}$ distribution was then binned and the resulting distribution of spacings was fit by the Brody distribution for different values of ω. The distribution of this new "averaged" set of energy levels is compared with Brody distributions for $\omega = 0.3$, 0.6, and 0.9 in Fig. 15. Although the statistics are limited so that one cannot determine a precise value of ω, values near 0.6 seem to provide a reasonable fit. This suggests that the 0^+ level spectrum is intermediate between ordered and chaotic in structure, providing another means of assessing future microscopic calculations.

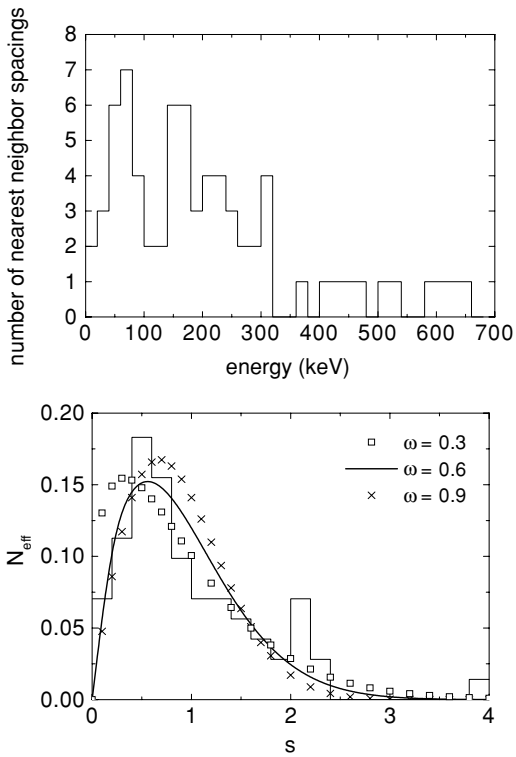

FIG. 15. (Top) Number of observed nearest neighbor spacings in the ensemble of nuclei studied, divided into 20-keV bins. (Bottom) Normalized nearest-neighbor spacings as a function of a dimensionless spacing variable, s, and fits with the Brody distribution for three values of ω. A binning of 0.2 in units of $N_{\rm eff}$ was used (see text).

IV. CONCLUSION

The present data more than double the number of 0^+ states previously known, and the variations in these data give rise to many questions. The number and excitation energy of 0^+ states varies considerably between nuclei. Even neighboring nuclei are quite different from each other, possibly indicating variations in the energies of noncollective states. However, often a large number of 0^+ states lie below the pairing gap and several occur as low in energy as $\sim$1200 keV. Many more 0^+ states exist than can be accounted with a simple estimation of the number and energies of double phonon excitations, but a more realistic estimate of the number of states can be made using the spdf-IBA. We also observe differences in the relative cross sections of the states. Some, such as those in the Gd isotopes, can be explained by phase-transitional behavior, but the trend of large cross sections around 1.5 MeV in most nuclei and around 3 MeV in ^{168}Er is intriguing. The number of low-lying 0^+ states peaks in the transition region where spherical and deformed states coexist in agreement with robust predictions of collective models. A statistical analysis of the distribution of 0^+ energies using the Brody distribution function suggests that the spectrum of these excitations is intermediate between ordered and chaotic in character. The variations in these data on 0^+ states provide a challenge to existing theories.

ACKNOWLEDGMENTS

We acknowledge helpful discussions with N. Lo Iudice, the help of Y. Alhassid in the statistical analysis, and IBA fits from E. A. McCutchan for two W isotopes that were not included in Ref. [20]. Research has been supported by the U.S. DOE under grant DE-FG02-91ER-40609, MLL, and DFG (C4-Gr894/2-3, Jo391/2-3).

[1] S. R. Lesher, A. Aprahamian, L. Trache, A. Oros-Peusquens, S. Deyliz, A. Gollwitzer, R. Hertenberger, B. D. Valnion, and G. Graw, Phys. Rev. C **66**, 051305(R) (2002).
[2] H.-F. Wirth *et al*., Phys. Rev. C **69**, 044310 (2004).
[3] N. Lo Iudice, A. V. Sushkov, and N. Yu. Shirikova, Phys. Rev. C **70**, 064316 (2004).
[4] N. Lo Iudice, International Workshop on *Symmetries and Low-Energy Phase Transitions in Nuclear Structure Physics*, Camerino, Italy, October 9–11, 2005, Universita degli Studi di Camerino, March; 2006.
[5] N. Lo Iudice, A. V. Sushkov, and N. Yu. Shirikova, Phys. Rev. C **72**, 034303 (2005).
[6] E. Zanotti, M. Bisenberger, R. Hertenberger, H. Kader, and G. Graw, Nucl. Instrum. Methods A **310**, 706 (1991).
[7] H.-F. Wirth *et al*., Beschleunigerlaboratium München Annual Report, 2000, p. 71.
[8] D. C. Radford, gf3: version 0.0. Modified by M. A. Caprio 2001.
[9] P. D. Kunz, CHUCK3, University of Colorado, unpublished.
[10] C. M. Perey and F. G. Perey, At. Data Nucl. Data Tables **17**, 1 (1976).
[11] D. A. Meyer *et al*., Phys. Lett. **B638**, 44 (2006).
[12] D. Bucurescu *et al*., Phys. Rev. C **73**, 064309 (2006).
[13] A. Spits *et al*., BLG 703 (1996), edited by A. Spits and P. H. M. Van Assche.
[14] N. V. Zamfir, Jing-ye Zhang, and R. F. Casten, Phys. Rev. C. **66**, 057303 (2002).
[15] Yang Sun, Ani Aprahamian, Jing-Ye Zhang, and Chinge-Tse Lee, Phys. Rev. C **68**, 061301(R) (2003).
[16] P. E. Garrett J. Phys. G **27**, R1 (2001).
[17] A. Aprahamian *et al*., Nucl. Phys. **A764**, 42 (2006).
[18] R. F. Casten and N. V. Zamfir, Phys. Rev. Lett. **87**, 052503 (2001).
[19] P. Debenham and N. M. Hintz, Nucl. Phys. **A195**, 385 (1972).
[20] Th. W. Elze, J. S. Boyno, and J. R. Huizenga, Nucl. Phys. **A187**, 473–480 (1972).
[21] E. A. McCutchan, N. V. Zamfir, and R. F. Casten, Phys. Rev. C **69**, 064306 (2004).
[22] O. Scholten, F. Iachello, and A. Arima, Ann. Phys. (NY) **115**, 325 (1978).
[23] N. V. Zamfir, P. von Brentano, R. F. Casten, and J. Jolie, Phys. Rev. C **66**, 021304(R) (2002).
[24] Pavel Cejnar and Jan Jolie, Phys. Rev. E **61**, 6237 (2000).
[25] F. Iachello and A. Arima, *The Interacting Boson Model* (Cambridge University Press, Cambridge, 1987).
[26] D. D. Warner and R. F. Casten, Phys. Rev. Lett. **48**, 1385 (1992).
[27] D. Tonev, A. Dewald, T. Klug, P. Petkov, J. Jolie, A. Fitzler, O. Moller, S. Heinze, P. von Brentano, and R. F. Casten, Phys. Rev. C **69**, 034334 (2004).
[28] E. A. McCutchan (private communication).
[29] D. Kusnezov, computer code OCTUPOLE.
[30] A. Bohr and B. R. Mottleson, *Nuclear Structure: Nuclear Deformations* (World Scientific, Singapore, 1998), Vol. 2.
[31] O. Bohigas and M. J. Giannoni, in *Mathematical and Computational Methods in Nuclear Physics*, edited by J. S. Dehesa, J. M. Gomez, and A. Polls (Springer-Verlag, Berlin, 1984).
[32] Y. Alhassid and A. Novoselsky, Phys. Rev. C **45**, 1677 (1992).